

Removal of Heavy Mineral from Mine Effluent with Amino Silica-Modified Magnetic Nanoparticles

Mahdi Jafari¹

¹*Department of Mining Engineering, Technical and Vocational University (TVU), Tehran, Iran,*

ABSTRACT

This study has examined the removal of metal ions of chromium (Cr), copper (Cu), lead (Pb), nickel (Ni), zinc (Zn), cobalt (Co), and cadmium (Cd) in the Gholleh Kaftaran lead mine effluent of Shahroud - Iran, with amino silica-modified magnetic nanoparticles. Adsorption has been proposed as a simple, economical, effective, and efficient method for removing heavy mineral ions from wastewater. In this study, magnetic nanoparticles were synthesized from co-precipitated iron ions II and III in the presence of ammonia, and then the nanoparticles were coated in ethanol/ammonia mixture using the sol-gel method. The structure of the synthesized nanoparticles was determined using the FT-IR, SEM, XRD, and ZETA methods. Various parameters such as pH of the solution, adsorbent dosage, stirring time, temperature, and initial concentration of metal ions were optimized. The maximum adsorption of metals by the adsorbent in optimal conditions occurred at the pH of 6, the adsorbent dose of 0.02 mg, the contact time of 60 minutes, the temperature of 25°C and the concentration of 20 ppm. Measurements of Cr, Cu, Pb, Ni, Zn, Co and Cd ions were performed by an inductively coupled plasma (ICP) device. The adsorption isotherms follow the Langmuir isotherm model for all heavy minerals except for Pb, which follows the Freundlich isotherm model. Overall, the results revealed that the adsorbent of amino-functionalized silica magnetic nanoparticles has a good performance for the removal of heavy mineral ions. The best adsorbent performance is related to Pb, while the weakest performance is related to Cu and Zn.

Key words: Silica, amino, heavy minerals, magnetic nanoparticles.

INTRODUCTION

Following an increase in population, modernity and welfare, many contaminants enter the environment, with toxic effects on the ecosystem. These contaminants include heavy minerals, which are important due to their harmful impacts on the environment, human health and safety (Li et al. 2013).

Heavy minerals have a specific gravity that is at least 5 times the specific gravity of water and are among the pollutants typically found in very small amounts in natural waters and in higher concentrations in mineral effluent, especially in metal mines. The main problem with heavy minerals is that they are not metabolized in the body and accumulate in body tissues, causing a variety of diseases. It is difficult to measure small and very small amounts of these metals by direct methods, so we need separation methods for their pre-concentration and measurement. Cr and Cd are major pollutants identified by the U.S. Environmental Protection Agency (Maity and Agrawal 2007).

Cd is very stable in the environment with a variety of inhalation effects including lung cancer, weakening of the immune system, and kidney damage. Among the heavy minerals found in nature, Cd monitoring is crucial as its concentration in the environment increases dramatically.

A variety of processes are used to remove heavy minerals, such as precipitation, membrane process, liquid-liquid extraction, solid phase extraction (SPE), flotation, adsorption etc. SPE through adsorption is the most widely used method for the removal of heavy minerals because it is cheaper and more effective than other methods. Conventional Cr and Cd removal methods are too costly, thus involving the development of new inexpensive and

economical methods (DeobandHafshejani et al. 2014).

Modified adsorbents are a new category of adsorbents introduced by researchers in recent decades to address the shortcomings of conventional adsorbents. Widely used adsorbents that have a good performance in removing pollutants from the aqueous environment are generally placed in two categories of modified adsorbents based on silica and ion imprinted polymers (IIPs).

Modified adsorbents include a broad range of materials consisting of organic, inorganic, highly natural and biopolymer structures. Modified adsorbents resulting from the functionalization of mesoporous silica are of great interest to researchers because of their high specific surface area, high porosity, controllability, and uniform pore sizes.

Removal heavy minerals from aqueous environments are very important. Because it is critical to prevent contamination of water resources due to the water crisis (Azouaou et al. 2010).

Some heavy minerals are essential for human life, while others not only do not play a positive role in the body's physiology, but may even be toxic in low concentrations. These metals result from human activities and some natural phenomena.

Vegetables have high capability to absorb and store heavy minerals; therefore, their consumption causes the accumulation of these substances in the body with adverse effects. Some industrial plants produce wastewater with heavy minerals and they lack treatment systems.

Over the last 50 years, humans have been increasingly exposed to heavy minerals, which can increase allergic reactions and cause genetic mutations. Therefore, developing reliable methods to determine Cr and Cd in the environment is of particular importance for public health and environmental pollution control (Boparai et al. 2013).

With this in mind, the present study is an attempt to remove heavy minerals (Cr, Cu, Pb, Ni, Zn, Co and Cd) from the Gholleh Kaftaran lead mine effluent of Shahroud with amino silica-modified magnetic nanoparticles.

Materials and Methods

Synthesis of magnetic nanoparticles

To synthesize magnetic nanoparticles using the co-precipitation method, 0.5 g of six-aqueous iron (III) chloride and 1 g of aqueous iron (II) chloride (in the 1:2 ratio) were weighed to which 50 ml of water was added. The resulting solution was exposed to ultrasonic waves for 30 minutes and then its contents were placed in a water bath at 50° C. while blowing nitrogen gas into the solution, 2 ml of ammonia was gradually added to it. The solution was then filtered and the precipitate was washed with water and ethanol and finally the resulting precipitate was dried (Abdolahinejad et al. 2015).

Modification of adsorbent with amino-functionalized silica

To increase the lifespan of nanoparticles and prevent their transformation to maghemite, the magnetite nanoparticles were coated with silica. This is done using two methods: (1) microemulsion and (2) sol-gel. The sol-gel method was used in this synthesis.

To modify the magnetite nanoparticles prepared above, 0.5 g of it was weighed and added to a mixture of 40 ml of ethanol and 1 ml of 25% ammonia solution. While the mixture was being stirred by magnetic stirrer, 0.5 ml of tetraethoxysilane (TEOS) and 1 ml of N-[3-(Trimethoxysilyl) propyl] ethylenediamine (TSD-NH₂) were added in ethanol.

The mixture was then stirred for 3 hours at 30° C for a period of 24 hours. Finally, the product was removed using a magnet, washed with ethanol and excess water, and dried at 80° C for 24 hours (Ketla et al. 2017).

(Fig. 1) shows a schema of the formation of iron oxide nanoparticles coated with silicas functionalized by amino-group.

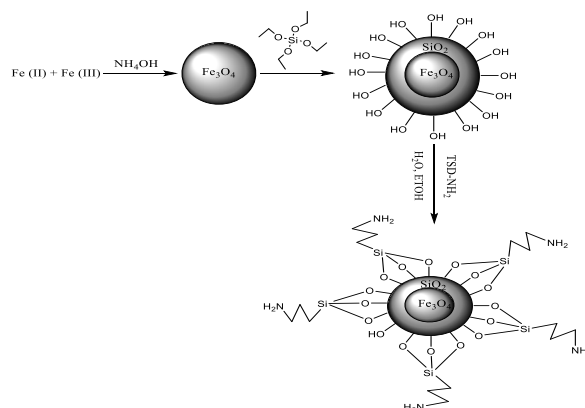


Fig. 1 Formation stages of amino silica-modified magnetic nanoparticles (Baig et al. 2015).

Preparation of solutions

The Gholleh Kaftaran lead Mine effluent of Shahroud was used in this study. Then to carry out the experiments, the mine effluent was diluted. To measure Cr, Cu, Pb, Ni, Zn, Co and Cd ions by the inductively coupled plasma (ICP) device, five standard solutions with concentrations of 2.5, 25, 250, 500, and 1000 micrograms per liter (ppb) were prepared through dilution with deionized water of the above standards.

Experiment procedure

First, to examine the adsorption of metal ions by the synthesized nanoadsorbent, 20 ml of a mixture of each of the ions of Cr, Cd, Cu, Pb, Ni, Co and Zn with a certain concentration was taken and poured in a 50 mL Erlenmeyer flask to which a certain dose of nanoadsorbent was added. The solution was stirred at a suitable temperature for a sufficient period of time. The magnetic nanoadsorbent was then separated by an external magnet. Since the solution poured into the ICP must be completely clear and free of any suspended solids, 10 ml of the metal ion solution was filtered through a filter paper and the remaining clear solution was decomposed using the ICP device to measure metal ions.

Results

In this section, the nanoadsorbent structure produced by infrared spectroscopy, scanning electron microscopy, X-ray diffraction spectroscopy and zeta potential methods were evaluated. Then, various parameters were examined to obtain the optimal conditions and achieve the highest adsorption efficiency. Finally, the isotherms of Langmuir, Freundlich, Tamkin and BET were examined.

Examining the adsorbent structure

The adsorbent used in this study was examined using the FT-IR, SEM, XRD, and Zeta potential spectroscopy methods.

Identification of magnetic silica nanoparticles using infrared spectroscopy

(Fig. 2) shows the FTIR adsorbent spectrum of amino-functionalized silicate magnetic nanoparticles to examine the functional groups present in its structure.

Examining the FTIR spectrum of the synthesized adsorbent indicates that three peaks are important to examine the structure of the synthesized magnetic nanoadsorbent. The stretching vibration of the Fe-O bond in the 579 cm⁻¹ region, which represents the magnetite phase, and the stretching vibration of the Si-O bond in the 1086 cm⁻¹ region, where the Fe-O-Si bond is not seen in the IR spectrum, because it appears in 574 cm⁻¹ and overlaps with the Fe - O bond.

The stretching vibration of the OH bond is shown in the 3437 cm⁻¹ region because of the adsorption of OH- by Fe₃O₄ nanoparticles. In addition, the spectral band of the NH functional group overlaps with the adsorption band of OH and is not observed.

The adsorption band located at 2924 cm⁻¹ is related to the C-H aliphatic stretching vibration of the hydrocarbon chain. Also, the adsorption band at 1632 cm⁻¹ is related to the bending vibration of the O-H group. The peak in the range of 1380 cm⁻¹ is related to C-N-H (Kalantari et al. 2019; Kampalanonwat and Supaphol 2014; Kumar and Rni 2013).

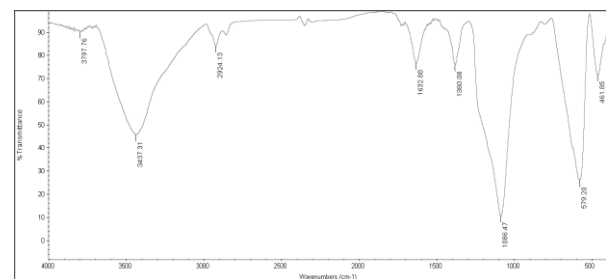


Fig. 2 FTIR spectrum of the synthesized adsorbent

Identification of magnetic silica nanoparticles using scanning electron microscopy

Several images were taken of the magnetic Nano adsorbents functionalized by scanning electron microscopy, some of which are shown in (Fig. 3).

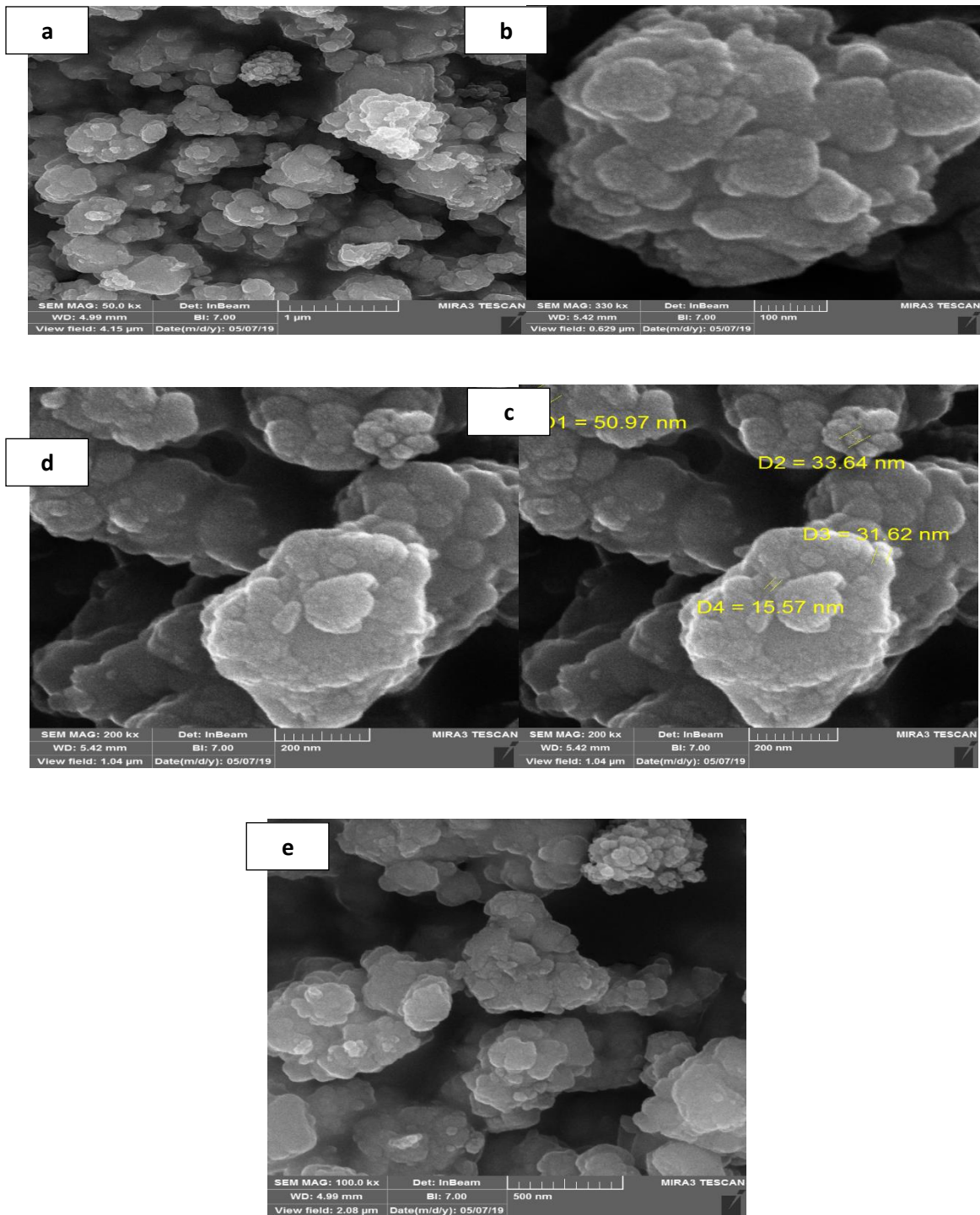


Fig. 3 Scanning electron microscope (SEM) images of the adsorbent sample a) 50x magnification b) 330x magnification c) 200x magnification d) 200x magnification with Nano sizing e) 200x magnification

The morphology of magnetic amino-functionalized silica nanoparticles was examined by the field emission scanning electron microscopy (FESEM), which is illustrated in (Fig. 3). (Fig. 3b) shows silica-coated and amino-functionalized iron oxide nanoparticles, where it is difficult to distinguish between magnetic nanoparticles and silica. However, it appears that the two nanoparticles have accumulated together and the agglomeration of the nanoparticles is visible. According to (Fig. 3d), the nanoparticle diameter is within the range of 15 to 60 nm. (Fig. 3e) shows a scale bar of 500 nm and a magnification of 100,000. Also, the two materials together show a unique morphology and particles below 100 nm are detectable ((Fig. 3c) with a scale

bar of 200 nm). Based on the definition of nano, the images confirm that the materials are nano. According to (Fig. 3), part of it is almost recognizable that nano structure has coated the amino-functionalized silica magnetic nanoparticles, which is consistent with the findings of other researchers (Attallah et al. 2017).

These researchers reported that silica had good interaction with the surface of iron oxide nanoparticles, and that a silica network is usually formed around the magnetic nanoparticles. This evidence confirms that magnetic amino-functionalized silica nanoparticles have been synthesized well (Kalantari et al. 2016).

Identification of magnetic silica nanoparticles using X-ray diffraction spectroscopy

(Fig. 4) shows the X-ray diffraction spectrum for the modified amino-functionalized magnetic adsorbent.

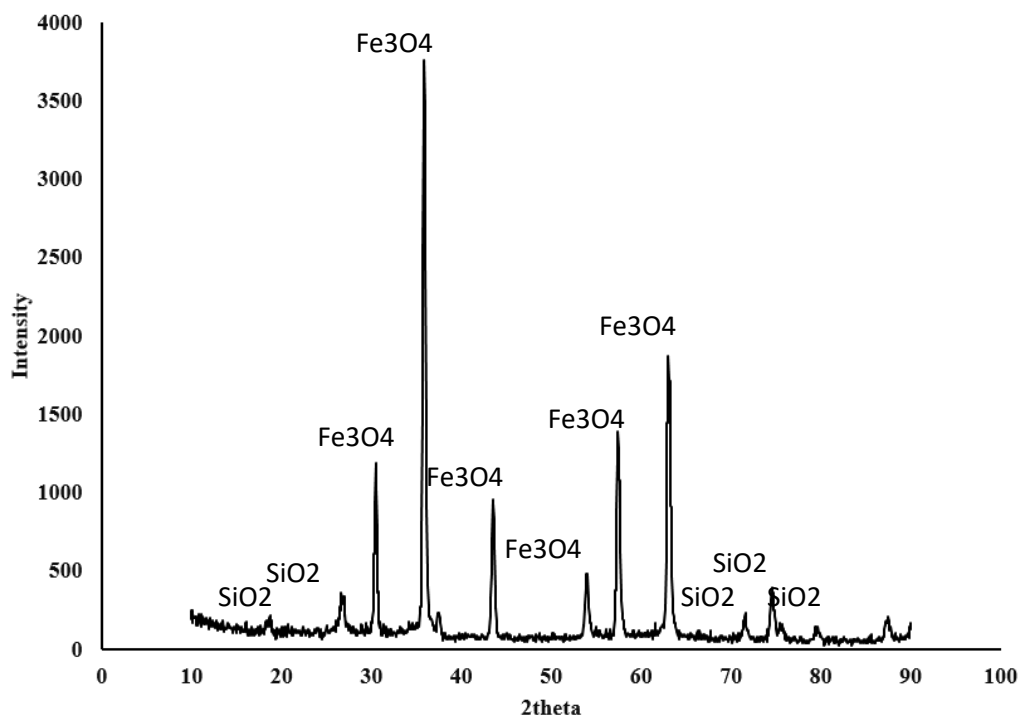


Fig. 4 X-ray diffraction image for the adsorbent sample

Phase identification is one of the most important applications of the XRD method. For this purpose, first the X-ray diffraction pattern was obtained from the sample and then the data were compared with the known standards to determine the phase of the sample. Examining (Fig. 4) and comparing the diffraction pattern obtained for Fe₃O₄ nanoparticles with the standards indicate the crystallization of the cubic spinel phase for the nanoparticles. As shown in the diffraction pattern for Fe₃O₄ nanoparticles,

silicate peak is also observed. (Fig. 4) clearly shows that the X-ray diffraction pattern for adsorbent nanostructures is a combination of Fe₃O₄ and SiO₂ nanoparticles. In other words, the crystal structure of Fe₃O₄ nanoparticles besides the SiO₂ around it has undergone a change.

Identification of magnetic nanoparticles using Zeta potential

If all the particles in the suspension have a negative or positive charge, then the particles will tend to repel each other and there will be no tendency for them to come together. The tendency of particles to repel each other is directly related to the zeta potential.

The most important factor in determining the size of the zeta potential is pH. In fact, the zeta potential quoted without a pH is completely meaningless. For example, a particle with a negative zeta potential is

in a suspension. If the suspension medium becomes more alkaline due to the addition of an additive, the particles will have fewer tendencies to come together, resulting in a more negative zeta potential. In the present study, the zeta potential result was estimated to be -14.9 mV, which indicates the negative charge of the adsorbent. Therefore, the adsorbent of the research can absorb positive metal ions. (Fig. 5) shows a design of the zeta potential test for the synthesized adsorbent sample.

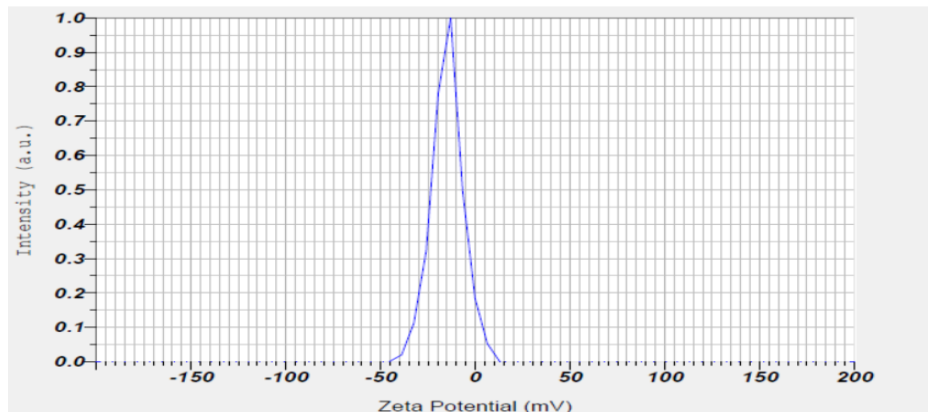


Fig. 5 Zeta potential image for the adsorbent sample

Examining the parameters affecting the removal rate

In this section, according to different conditions and the nature of the functional groups, parameters such as pH of the solution, adsorbent dose, contact time, initial concentration of metal ions, and temperature were examined.

Effect of pH of the solution on removal of metal ions

To examine the effect of pH on the adsorption efficiency of metal ions by the synthesized magnetic adsorbent, the pH of solutions 2, 4, 5, 6 and 8 was adjusted. (Fig. 6) shows the effect of pH on the removal of heavy minerals by Nano adsorbents.

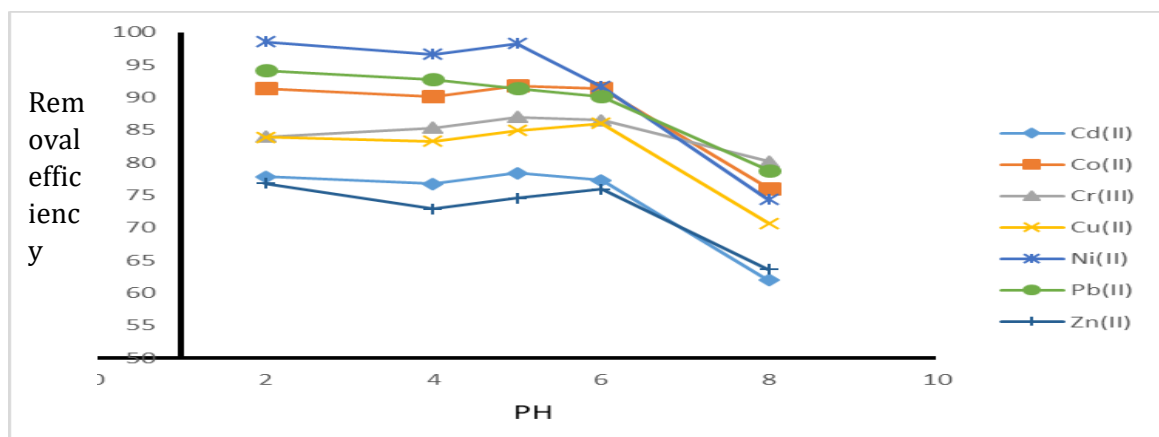


Fig. 6 The effect of pH on the removal of heavy minerals

According to the results presented in (Fig. 6), the adsorption efficiency has increased and then decreased at pH 5 to 6. As the pH has increased, the amount of positive hydrogen ions in the water has decreased. This means an increase in OH⁻ ions. Therefore, an increase in the OH⁻ ions has led to the reaction of this ion with the positive ions of the heavy mineral and suspended the heavy minerals as a solid phase in solution. Therefore, an increase in the pH affects the metal adsorption and reduces the adsorption efficiency.

Effect of adsorbent dose on the removal of metal ions

To examine the effect of adsorbent dose on adsorption efficiency, 5, 10, 20, 40 and 60 mg of adsorbent were added to the solution of metal ions. After they were mixed at the right time, the adsorbent was separated from the solution using a magnet and the concentration of metal ions was measured using the ICP device. (Fig. 7) shows the results of the effect of the adsorbent dose on the removal of heavy minerals.

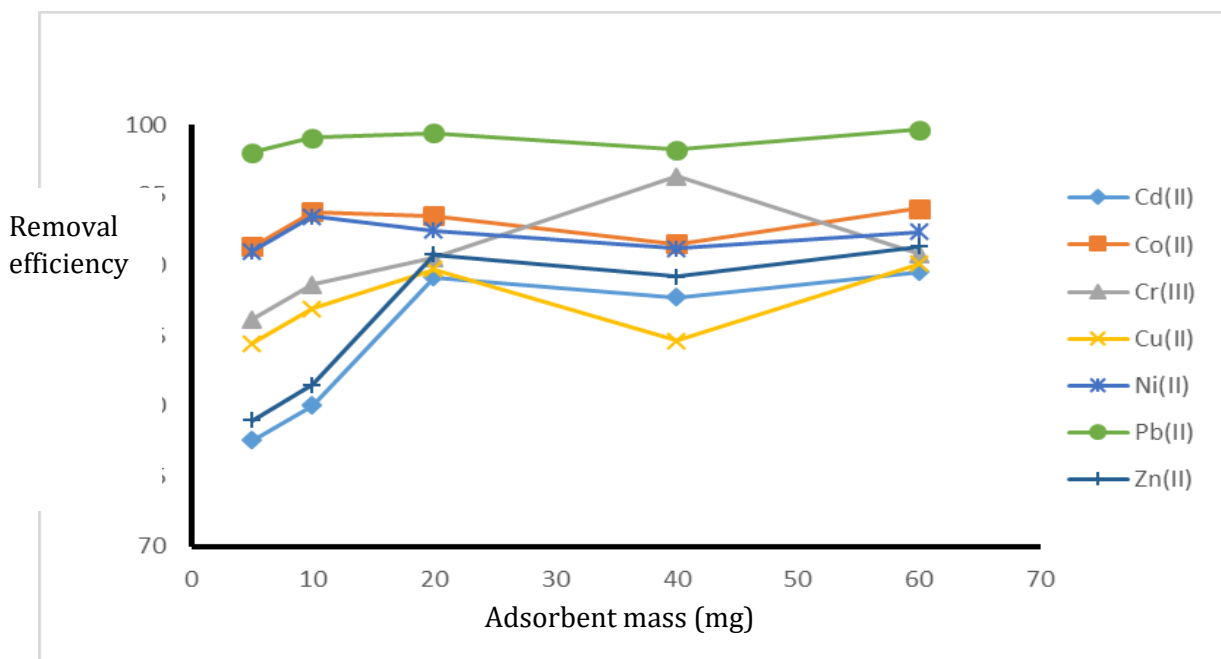


Fig. 7 Effect of adsorbent dose on the removal efficiency of heavy minerals

The results presented in (Fig. 7) show that the adsorption efficiency increases due to an increase in the adsorbent dose. An increase in the adsorbent dose increases the contact between the adsorbent particles and the metal ions, which in turn increases the efficiency. However, if the concentration of heavy minerals in the sample is constant, the excessive increase of the adsorbent has little effect on the efficiency.

Effect of time on the removal of metal ions

To identify the effect of the contact time of adsorbent with the solution of metal ions on the adsorption efficiency, the contact times of 5, 10, 30, 60, 90 and 180 minutes were examined. (Fig. 8) shows the effect of time on the removal efficiency of heavy minerals.

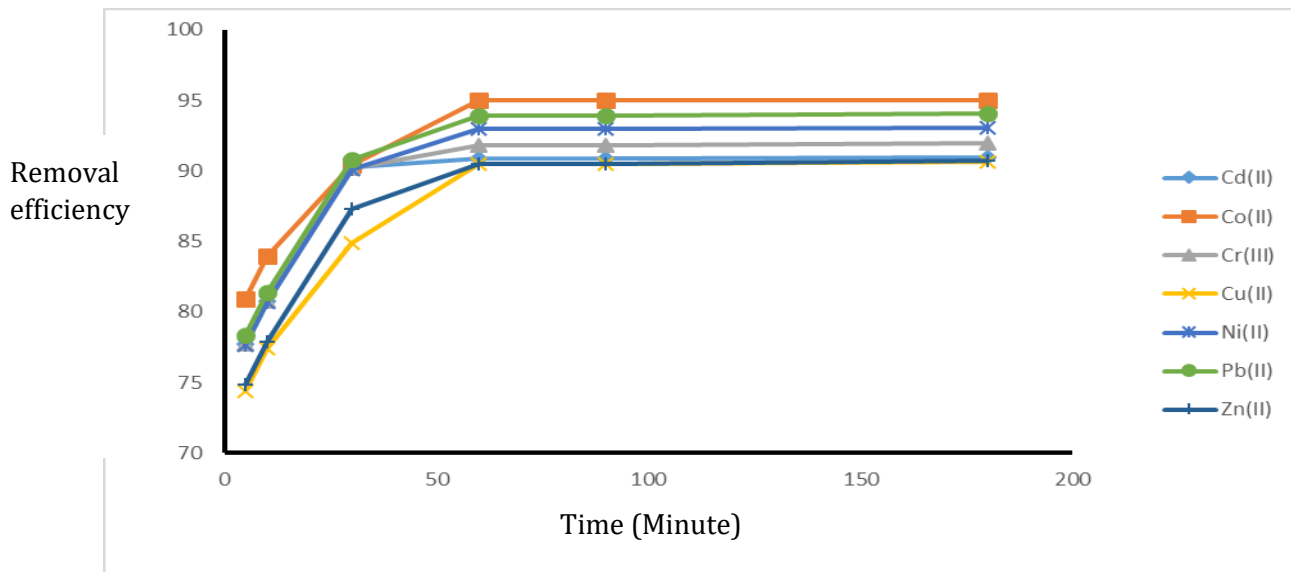


Fig. 8 The effect of time on the removal of heavy minerals

The adsorption rate of metal ions is related to the efficiency of the adsorbent and the activity of the metal, and therefore determines the residence time of the adsorbent at the solid-solution interface. Adsorption time profiles were examined by performing discontinuous adsorption experiments. The results presented in (Fig. 8) shows an increase in the adsorption efficiency due to an increase in time, and the increased time increases the contact between metal ions and the adsorbent. The results show that the adsorption rate for heavy minerals is constant at times longer than 50 minutes. In other

words, an excessive increase in the adsorption time reduces the adsorbent efficiency in heavy mineral adsorption.

Effect of initial concentration on ion removal rate

To identify the initial concentration on the adsorption efficiency, concentrations of 5, 10, 20, 50, 100, and 200 ppb were examined. (Fig. 9) shows the effect of the initial concentration on the removal efficiency of heavy minerals.

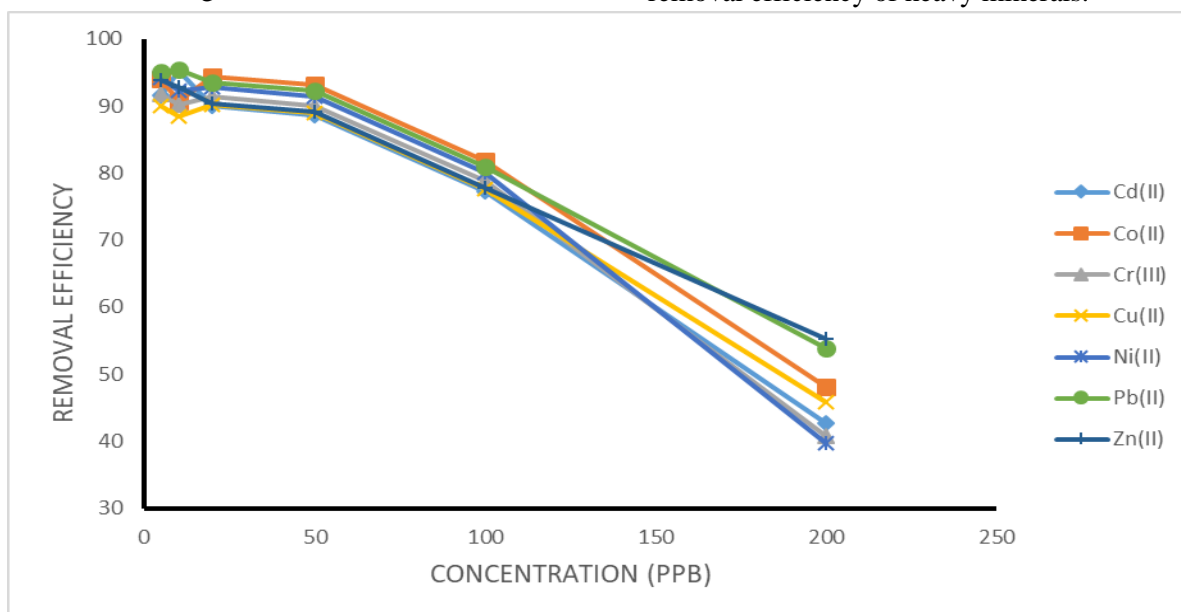


Fig. 9 Effects of initial concentration on the removal of heavy minerals

The results presented in (Fig. 9) show that an increase in the initial concentration in the rate of constant adsorbent leads to a decrease in adsorption efficiency. At high concentrations, large amounts of metal ions reduce the contact of ions with the adsorbent, which decreases the adsorption efficiency.

Effect of temperature on the ion removal rate

To identify the effect of temperature on the adsorption efficiency, temperatures of 25, 35 and 45 degrees centigrade were examined. (Fig. 10) shows the effects of temperature on the removal of heavy minerals. According to the results presented

in this figure, an increase in the temperature in all cases except for Cd, Co and Ni has little effect on the adsorption efficiency. In Cr and Ni, the increase in temperature leads to an increase in the removal of heavy minerals, while in Co, an increase in temperature decreases the adsorption efficiency. An increase in temperature leads to an increase in molecular motions. Increased molecular motion can increase the contact of metal ions with Ni and Cd metals and, ultimately, increase the adsorption efficiency. On the other hand, an increase in the temperature increases the oxygen concentration of water, which causes Cd to react with oxygen. This ultimately reduces the adsorption efficiency by creating a solid phase.

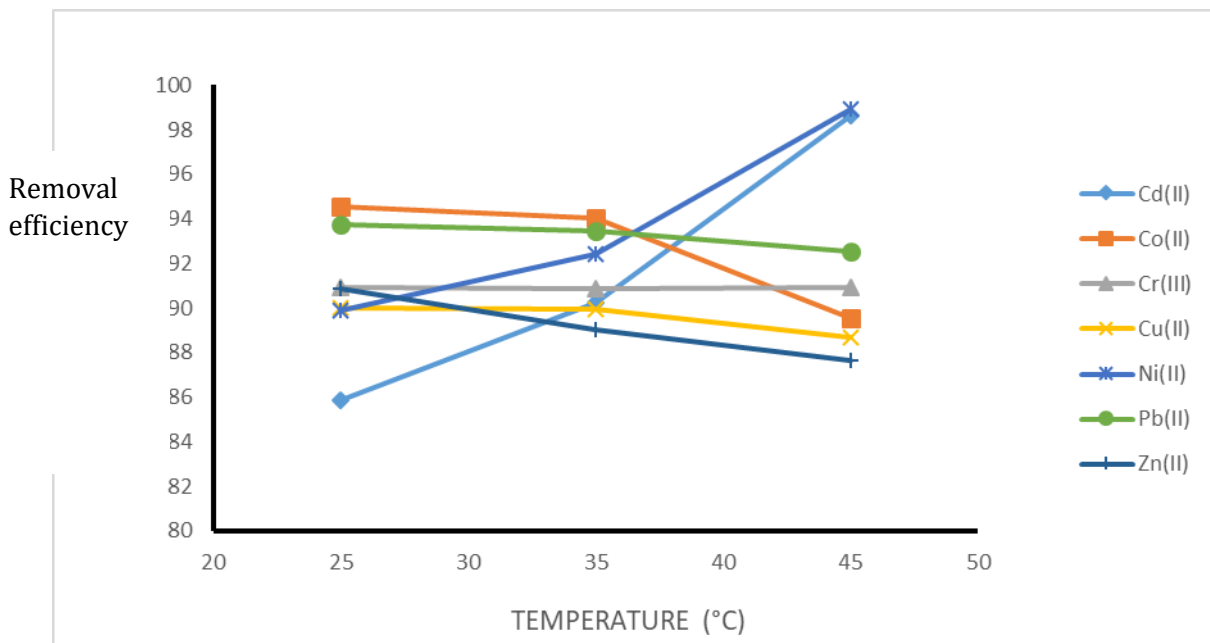


Fig. 10 Effects of temperature on the removal of heavy minerals

Standard curves

(Table 1) shows the standard curve data. (Fig. 11) shows the standard curve for different heavy mineral samples, regression results and error for different samples.

Table 1 Standard curve results

Ion	R ²	Standard curve equation	Mean error
Cd (II)	0.9988	y = 2.3382x - 20.139	1.093
Co (II)	0.9974	y = 0.8948x + 34.314	-0.939
Cr (III)	0.9973	y = 1.5467x + 42.659	-0.604
Cu (II)	0.9966	y = 0.7959x + 32.253	-1.586
Ni (II)	0.9985	y = 0.6001x + 15.41	-0.609
Pb (II)	0.9919	y = 0.1906x + 9.9736	1.180
Zn (II)	0.9920	y = 5.0147x + 98.845	-1.660

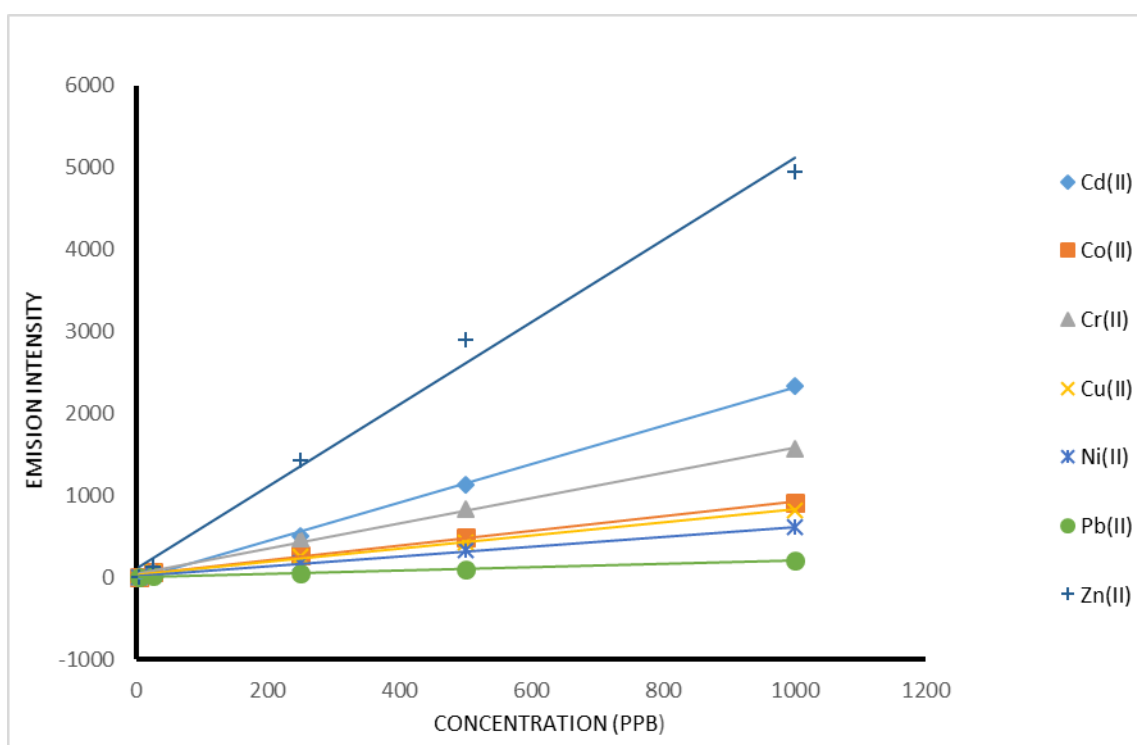


Fig. 11 Standard curves of heavy minerals

The results show that the calibration curves in different samples are linear. These equations are shown in (Fig. 11) and the regression rate of these curves is more than 99%. Therefore, the equations have been calculated accurately with an accuracy of less than 1%.

Examining adsorption isotherms

The agreement of the adsorption equilibrium experimental data with the Langmuir, Freundlich, Tamkin, and BET adsorption isotherm models was examined using Equations 1 to 5, respectively.

$$\frac{c_e}{q_e} = \frac{1}{ab} + \frac{1}{a}c_e \quad (1)$$

$$\ln q_e = \ln k_f + \frac{1}{n}(\ln c_e) \quad (2)$$

$$q_e = B \ln C_e + C \quad (3)$$

$$\ln q_e = A \ln C_e + B \quad (4)$$

$$q_e = \frac{(C_0 - C_e)}{m} \times V \quad (5)$$

It should be noted that the isotherm indicators are:

C_e : Equilibrium concentration of adsorbate (mg/L)

q_e : Mass of adsorbate per unit mass of adsorbent (mg/g)

k_f : Freundlich isotherm constant (dimensionless)

a and b : Langmuir isotherm constants (dimensionless)

B : Constant of Tamkin and BET

n : Constant of metal adsorption

m : adsorbent mass (g)

V : Reactor volume (L)

C_0 : Initial concentration (mg/L)

The results presented in (Table 2) show that all heavy minerals follow the Langmuir adsorption isotherm except for Pb, which follows the Freundlich adsorption isotherm.

Table 2. Results of Cd isotherm

Heavy mineral	q_e	C_e	Langmuir				Freundlich				Tamkin				BET				
			R ²	err	a	b	R ²	err	k	n	R ²	err	B	C	R ²	err	A	B	
Cd	22.5	0.9	0.99	0.01	1.3	43.86	0.88	0.12	24.84	3.32	0.91	0.09	8/25	25.1	0.71	0.29	5.98	-18	
	32	1.6			3								83						.0
	33.75	2.7											3						8
	37.5	4.5																	
Co	16.67	0.5	0.97	0.03	0.8	47.66	0.94	0.06	26.86	2.27	0.94	0.06	9/88	21.15	0.91	0.09	3.74	10	
	16	0.8																	
	27.14	1.9																	
	35.45	3.9																	
Cr	16	0.8	0.99	0.01	0.9	35.58	0.96	0.04	25.33	2.527	0.98	0.02	7/44	17.71	0.81	0.19	5.14	-13	
	21.43	1.5			4														.4
	23.63	2.6											1						9
	29.3	4.4																	
Co	16.67	0.5	0.97	0.03	0.8	47.66	0.94	0.06	26.86	2.27	0.94	0.06	9/88	21.15	0.91	0.09	3.74	10	
	16	0.8																	
	27.14	1.9																	
	35.45	3.9																	

Cu	14	0.7	0.	0.	0.	30.30	0.89	0.1	32.	3.1	0.8	0.1	5.	15	0.	0.	6.	-
	18.89	1.7	94	06	9			1	26		6	4	62	.3	89	11	88	17
	17.86	2.5												5				.6
	25.79	4.9																7
Ni	22.5	0.9	0.	0.	5.	26.88	0.33	0.6	33.	3.6	0.3	0.6	0.	-	0.	0.	8.	-
	21.43	1.5	99	01	3			7	62	8	5	5	15	3.	25	75	10	23
	27.14	1.9			1									18				.4
	25.79	4.9																4
Pb	16	0.8	0.	0.	0.	60.97	0.91	0.0	25.	2.5	0.8	0.1	13	16	0.	0.	2.	-
	18.89	1.7	76	24	3			9	11	4	5	5	.5	.9	89	11	92	7.
	33.75	2.7			7								9	8				03
	35.45	3.9																
Zn	14	0.7	0.	0.	1.	28.9	0.69	0.3	24.	2.3	0.6	0.3	6.	18	0.	0.	3.	-
	27.14	1.9	97	03	9			1	55	6	7	3	04	.3	43	57	83	9.
	23.63	2.6			8									5				31
	25.79	4.9																

Conclusion

- XRD results show that the comparison of the diffraction pattern obtained for Fe₃O₄ nanoparticles and its comparison with the standards indicate the crystallization of the cubic spinel phase for the nanoparticles. As shown in the diffraction pattern for Fe₃O₄ nanoparticles, silicate peak is also observed.
- According to the results presented in the figure, an increase in the pH decreases the adsorption efficiency. As the pH increases, the amount of positive hydrogen ions in the water decreases. This means an increase in OH⁻ ions. Therefore, an increase in the OH⁻ ions leads to the reaction of this ion with the positive ions of the heavy mineral and suspends the heavy minerals as a solid phase in solution. Therefore, an increase in the pH of the metal disrupts the adsorption and reduces the adsorption efficiency.
- An increase in the adsorbent dose increases the contact between the adsorbent particles and metal ions, which increases the efficiency. However, if the concentration of heavy minerals in the sample is constant, an excessive increase of the adsorbent has little effect on the efficiency.
- An increase in the efficiency time leads to an increase in the adsorption rate, which in turn increases the contact between the metal ions and the adsorbent.
- At high concentrations, large amounts of metal ions reduce the contact of ions with the adsorbent, which decreases the adsorption efficiency.
- In Cr and Ni, an increase in the temperature leads to an increase in the removal of heavy minerals, while in Co, an increase in the temperature decreases the adsorption efficiency. An increase in the temperature leads to an increase in molecular motion. Increased molecular motion can increase the contact of metal ions with Ni and Cd metals and ultimately increase the adsorption efficiency. On the other hand, an increase in the temperature leads to an increase in the oxygen concentration of water and this causes Cd to react with oxygen and ultimately reduces the adsorption efficiency by creating a solid phase.
- The results presented in (Fig. 6) show that the best adsorption efficiency at low pH is related to Ni and Pb, and that an increase in the pH improves the adsorption efficiency of Cr and Pb. As shown in (Fig. 7), the highest adsorption efficiency is related to Pb, which is significantly better than other metals. (Fig. 8) shows the best adsorption efficiencies for Co and Pb. According to this figure, there is no

significant difference between the adsorption efficiency of Co and Pb. According to (Fig. 9), the best adsorption efficiency belongs to Pb, although other metals are not significantly different from Pb (at low concentrations). However, at high concentrations of heavy mineral, Pb adsorption is significantly better than other metals (except Ni). Therefore, according to the results, this adsorbent has the best efficiency for Pb removal.

- The results presented in (Table 2) show that Zn and Cu are at the lowest level of adsorption efficiency. Therefore, this adsorbent has the least effect on the adsorption of Zn and Cu metals.
- The adsorption isotherms of all heavy minerals follow the Langmuir isotherm model, except for Pb, which follows the Freundlich isotherm model.

References

- Li Y, Zhu S, Liu Q, Chen Z, Gu J, Zhu C, et al. (2013) Ndoped porous carbon with magnetic particles formed in situ for enhanced Cr(VI) removal. *Water Res* 47(12): 4188-97. <https://doi.org/10.1016/j.watres.2012.10.056>
- Maity D, Agrawal DC (2007) Synthesis of iron oxide nanoparticles under oxidizing environment and their stabilization in aqueous and non-aqueous media. *Journal of Magnetism and Magnetic Materials* 308: 46–55. <https://doi.org/10.1016/j.jmmm.2006.05.001>
- DeobandHafshejani L, Mortazavi Ghanavati P, Sabzalipour S, Boroumand Nasab S (2014) Study of kinetics and patterns of chromium adsorption of six volumes from aqueous media by nanoparticles of ash leaves of the tree. *Irrigation Engineering Journal* 36 (1): 31-23.
- Azouaou N, Sadaoui Z, Djaafri A, Mokaddem, H (2010) Adsorption of cadmium from aqueous solution onto untreated coffee grounds: equilibrium, kinetics and thermodynamics. *Journal of Hazardous Materials* 184(1–3): 126–134. <https://doi.org/10.1016/j.jhazmat.2010.08.014>
- Boparai H K, Joseph M, O'Carroll D M (2013) Cadmium (Cd²⁺) removal by nano zerovalent iron: surface analysis, effects of solution chemistry and surface complexation modeling. *Environmental Science and Pollution Research* 20(9): 6210–6221
- Abdolahinejad S, Barghi M, Siedi M (2015) Removal of six volumes of chromium by ferrite nanoparticles. *Journal of Chemistry and Chemical Engineering of Iran* 34 (1): 37-29.
- Ketla B, Taddese AM, Yadav O.P, Diaz I, Mayoral A (2017) Nano –crystalline titanium (IV) tungstomolybdate cation exchanger: Synthesis, characterization and ion exchange properties. *Chemical Engineering Journal* 262: 597–606. <https://doi.org/10.1016/j.cej.2017.01.018>
- Baig U, Rao R, Khan A, Sangi M, Gondal M (2015) Removal of carcinogenic hexavalent chromium from aqueous solutions using newly synthesized and characterized polypyrrole–titanium(IV) phosphate nanocomposite. *Chemical Engineering Journal* 280: 494-504. <https://doi.org/10.1016/j.cej.2015.06.031>
- Kalantari R, Karbasi A, Fathi S (2016) Comparison of heavy mineral adsorption of chromium from water solutions using magnetic nanoparticles. *Journal of Environmental Science and Engineering* 5 (8): 18-13.
- Kampalanonwat P, Supaphol P (2014) The Study of Competitive Adsorption of Heavy mineral Ions from Aqueous Solution by Aminated Polyacrylonitrile Nanofiber Mats. *Eco-Energy and Materials Science and Engineering* 56: 142-151. <https://doi.org/10.1016/j.egypro.2014.07.142>
- Kumar H, Rni R (2013) Structural Characterization of Silver Nanoparticles Synthesized by Micro emulsion Route. *International Journal of Engineering and Innovative Technology (IJEIT)* 3(3): 2277-3754
- Attallah OA, Al-Ghobashy MA, Nebsen M, Salem MY (2017) Removal of cationic and anionic dyes from aqueous solution with magnetite/pectin and magnetite/silica/pectin hybrid nanocomposites: kinetic, isotherm and mechanism analysis. *RSC Advances*. 6(14), 11461-11480. <https://doi.org/10.1039/C5RA23452B>